Acetylation of Bacterial Cellulose Using N-Methyl-imidazole as a Catalyst Under Solvent-free and N,N-dimethylacetamide/Lithium Chloride Solvent Systems

Jian Wu,[a] Yanlei Tao,[a] Alei Geng,[a,b] Rongrong Xie,[a] Daochen Zhu,[a] Qianqian Wang,[a] Lushan Sun,[c,*] and Jianzhong Sun [a,*]

Bacterial cellulose acetate (BCA) at a low degree of substitution (DS) was prepared using acetic anhydride in the presence of N-methylimidazole (NMIM) as a catalyst. The acetylated reaction was studied in both solvent-free (heterogeneous) and N,N-dimethylacetamide/lithium chloride (DMAc/LiCl; homogeneous) systems, where the DS ranges of BCA obtained from heterogeneous (BCA-HE) and homogeneous (BCA-HO) systems were recorded as 0.31 to 0.95 and 0.4 to 1.5, respectively. The DS values could be effectively controlled by adjusting the reaction conditions. Compared to the heterogeneous reaction, the homogeneous reaction could be processed under a mild condition within a short time. The BCA-HE and BCA-HO displayed good water solubility at a DS value less than 0.95 and 1.09, respectively. The structural and the characteristic changes were confirmed by scanning electron microscopy, Fourier transform infrared, X-ray diffraction, ^{13}C cross-polarization magic angle spinning nuclear magnetic resonance, and thermogravimetric analyses. The present study may offer a convenient, mild, and green catalyzed-processing to tailor low DS of cellulose acetate.

Keywords: Bacterial cellulose; Acetylation; N-methylimidazole; Structure analysis; Heterogeneous and homogeneous reactions

Contact information: a: Biofuels Institute, School of the Environment and Safety Engineering, Jiangsu University, Zhenjiang 212013, Jiangsu, China; b: Jiangsu Key Laboratory for Biomass Energy and Material, Nanjing 210042, Jiangsu, China; c: Institute of Textiles and Clothing, The Hong Kong Polytechnic University, Hong Kong, China;
** Corresponding authors: jzsun1002@ujs.edu.cn; Sarina.sun@polyu.edu.hk*

INTRODUCTION

Cellulose is one of the most abundant renewable biopolymers in the world. It could substitute for fossil feedstocks when manufacturing high-value chemicals and energy products, and it is obtained from renewable resources such as plants and microorganisms (Klemm *et al*. 2005; Sheldon 2014; Isikgor and Becer 2015). In recent years, bacterial cellulose (BC) has gained much attention due to its unique physical properties; it has an ultrafine 3D network structure of cellulose nanofibers with a high purity, high crystallinity, Young's modulus, tensile strength, and water-holding capacity. As a natural polymer, it also exhibits a good biocompatibility and biodegradation properties. The BC has shown a great potential as a versatile nanomaterial that offers a wide range of applications in diverse industrial fields, such as food, papermaking, electronics, textile, and biomaterials (Svensson *et al*. 2005; Fu *et al*. 2013; Shah *et al*. 2013; Nie *et al*. 2014; Shi *et al*. 2014).

It is well known that cellulose is a type of homo-polysaccharide composed of β-1,4-linked D-glucopyranosyl residues, which is rich in hydroxyl groups and shows high hydrophilicity. However, it is difficult to dissolve cellulose in water and conventional organic solvents due to the intra- and intermolecular hydrogen bonding and its high

polymerization degree (Klemm *et al*. 2005; Cao *et al*. 2016a). Therefore, the chemical modification of cellulose, such as esterification, etherification, and graft copolymerization (Kim *et al*. 2002; Wang *et al*. 2007; Fox *et al*. 2011; Amin *et al*. 2015; Kang *et al*. 2015), has gained much attention. Among the various chemical modifications available, cellulose acetylation is one of the effective methods, where the hydrophilic hydroxyl groups of cellulose are replaced by hydrophobic acetyl groups at the C-2, C-3, and C-6 positions of the anhydroglucose units (AGU) (Kim *et al*. 2002). The products of cellulose acetate (CA) are considered important derivatives in commercial application (Fischer *et al*. 2008). The CA can be classified into cellulose triacetates, diacetates, and monoacetates according to the degree of substitution (DS) values. Cellulose triacetate with high DS (> 2.8) has been used in many fields, such as textile fibers, medical, and pharmaceutical products. The dry spun cellulose diacetate (DS > 2.0) is the most widely used form of CA in the cigarette industry. In general, cellulose monoacetates with a low DS value (< 1.5) would exhibit water solubility for some important industrial applications, such as thickening, lubricating, and stabilizing (Buchanan *et al*. 1991; Wheatley 2007; Cao *et al*. 2016a) properties.

The CA is generally prepared by the reaction involving the functional hydroxyl group with acetic anhydride (Ac_2O) under heterogeneous or homogeneous conditions (Frisoni *et al*. 2001; Ass *et al*. 2004; Cetin *et al*. 2009; Ashori *et al*. 2014). Until recently, it mainly has been produced in the textile industry by the heterogeneous acetic acid processes, in which cellulose is first swelled in acetic acid and then acetylated with sulfuric acid as catalyst in the presence of Ac_2O. Although sulfuric acid shows good catalytic activity for production of CA, there are obviously some drawbacks associated with this process that encourage side reactions and considerable corrosion or poisoning effects (Li *et al*. 2009; Hu *et al*. 2011; Asaadi *et al*. 2018). Therefore, a variety of other catalysts have been explored for acetylating cellulose, including perchloric acid, pyridine, α-hydroxy acids, iodine, and ionic liquids (ILs) (Lin *et al*. 2011; Zhou *et al*. 2016; Ávila Ramírez *et al*. 2016a,b, 2017).

It is worth noting that N-methylimidazole (NMIM), which is an excellent catalyst, has been applied in acetylation of plant polysaccharide in dimethyl sulfoxide (DMSO) as solvent system, such as in the cell wall, xylan, and eucalyptus woods (Lu and Ralph 2003; Zhang *et al*. 2012a, 2016). Imidazole has also been developed for the acetylation of microcrystalline cellulose in the N,N-dimethylacetamide/lithium chloride (DMAc/LiCl) system (Nawaz *et al*. 2013; Pires *et al*. 2015). The NMIM-based ILs can function both as a catalyst and as solvent for cellulose acetylation (Cao *et al*. 2007; Pang *et al*. 2016). The NMIM has presented a competitive ability in catalytic acetylation due to its low cost, mild reactivity, and less toxicity.

In the past decade, along with the solvents engineering technology to be developed, the homogeneous reaction is currently proposed through dissolving the cellulose in some suitable non-aqueous solvents. With these new solvents, this approach has shown some advantages over the heterogeneous reaction, where the DS values of CA can be effectively controlled, and more evenly distributed acetate groups can be introduced along the cellulose chain (Wu *et al*. 2004; Zhu *et al*. 2006; Cao *et al*. 2007; Sun *et al*. 2013; Zhang *et al*. 2013; Tian *et al*. 2014). At present, the most commonly used solvents are ILs and DMAc/LiCl for dissolving the cellulose to promote homogeneous acetylated modification. The ILs have an intrinsically high cost and are a viscous solvent. In contrast, DMAc/LiCl is relatively cheap and possesses lower solution viscosity. Especially, the lower solution viscosity favors the reaction due to the concomitant increase in reagent diffusion coefficient (Lima *et al*. 2011; Zhang *et al*. 2012b; Nawaz *et al*. 2013; Wang *et al*. 2017). Therefore, DMAc/LiCl has become a preferred solvent to be selected in the homogeneous acetylation

of cellulose (Ass *et al*. 2006a, 2006b; Lima *et al*. 2011; Wan *et al*. 2017).

In this paper, a comparison study for NMIM-catalyzed BC acetylation was developed under solvent-free (heterogeneous) and DMAc/LiCl (homogeneous) systems in the presence of Ac_2O as the acetylating agent. The main purpose of this study is to investigate the relevant key variables involved in tailoring the BCA at a desired DS value. In addition, the morphology, structure, and properties associated with the produced BCA were observed and analyzed using scanning electron microscopy (SEM), Fourier transform infrared (FTIR) spectroscopy, ^{13}C cross-polarization/magic angle spinning nuclear magnetic resonance (^{13}C CP/MAS NMR), X-ray diffraction (XRD), and thermogravimetric analysis (TGA). These efforts will assist in the evaluation of the BC acetylation using NMIM as catalyst under various solvent systems.

EXPERIMENTAL

Materials

The reagents NMIM and Ac_2O were purchased from Sigma–Aldrich (Shanghai, China). The DMAc, lithium chloride ($LiCl·H_2O$), and other chemicals used were of analytical grade and commercially available from Sinopharm Chemical Reagent Co., Ltd. (Shanghai, China). The $LiCl·H_2O$ was dried under vacuum for 4 h at 115 °C prior to use.

Methods

BC preparation

The *Gluconacetobacter xylinus* ATCC53582 strain was utilized in this study. Bacterial cellulose was produced by *G. xylinus* ATCC53582 under static culture in Hestrin-Schramm liquid medium (Hestrin and Schramm 1954). The medium (w/v) was composed of 2% glucose, 0.5% peptone, 0.5% yeast extract, 0.27% Na_2HPO_4, and 0.115% citric acid in distilled water (pH 6.5). The fermentation process was performed at 30 °C during seven days. The obtained BC membranes were placed in 1% NaOH solution (w/v) for 24 h to remove bacteria, and then thoroughly washed with deionized water to obtain neutral solutions. The purified BC membrane was freeze-dried and ground into powder of the 40-mesh size.

The acetylation of BC

For preparation of heterogeneous BCA (BCA-HE), the reaction conditions were optimized as continuous magnetic agitation in an oil bath using 0.1 g dry BC (0.1 g dry BC, corresponding to 0.62 mmol AGU). The BC powder was dispersed in a desired amount of Ac_2O (8, 9, 10, 11, and 12 mL) solution, and various concentrations of NMIN (0.1, 0.2, 0.3, 0.4, and 0.5 mM) were subsequently added to the reaction solution. The reaction was performed at a chosen temperature (50, 60, 70, 80, and 90 °C) for different time intervals (180, 240, 300, 360, and 420 min). After the reaction was finished, the products were washed with ethanol three times and subsequently washed with deionized water to make it neutral. Finally, the product was freeze-dried.

For preparing homogeneous BCA (BCA-HO), initially, the DMAc/LiCl (91/9, W/W) solution was prepared by adding dried $LiCl·H_2O$ into DMAc (Zhang *et al*. 2012b). The mixture was heated at 110 °C until LiCl was completely dissolved. Next, 0.1 g of BC was mixed with 10 mL of DMAc/LiCl solution, and the mixture was stirred for 3 h at 80 °C when a transparent BC solution was obtained and then allowed to cool to the room temperature. At that time, the Ac_2O (1 to 5 mL) and NMIM (0.1 to 0.5 mM) were added,

and the reaction was conducted at various time intervals (30 to 150 min) and temperatures (20 to 60 °C). The products were precipitated in deionized water, washed with ethanol three times, and then washed with deionized water. Finally, the BCA-HO was obtained after lyophilization for further study.

Determination of DS and water solubility

The DS is defined as the average number of sites per glucose unit that posses a substituent group. The DS was determined by the back titration method, which involved the complete basic hydrolysis of the ester linkages using excess alkali. Briefly, the freeze-dried acetylated cellulose was added to 40 mL of 75% ethanol in a flask and heated at 60 °C for 30 min. Subsequently, it was cooled to room temperature and 40 mL of 0.1 M NaOH solution was added to the flask. Then the reaction mixture was heated for 15 min at 60 °C and then 48 h at room temperature. The excess alkali was back-titrated with 0.1 M HCl using phenolphthalein as an indicator (Kim *et al*. 2002; Zhou *et al*. 2016). The original unmodified cellulose was used as a blank.

The DS was calculated according to the standard test method for cellulose acetate ASTM D871-96 (2004) (Zhou *et al*. 2016). The DS value was calculated using Eqs. 1 and 2,

$$A\ (\%) = [(V^0_{HCl} - V_{HCl})]M \times 43 \times 100 / w \quad (1)$$

$$DS = 162 \times A / [4300 - 42 \times A] \quad (2)$$

where A is the percentage (%) of acetyl groups in the sample, V^0_{HCl} is the volume (mL) of HCl used to titrate blank, V_{HCl} is the volume (mL) of HCl used to titrate sample, M is the molarity concentration (mol/L) of used HCl solution and the NaOH solution (0.1 M in this paper for both solutions), w is the sample amount (g) as dry substance, 43 is the molecular weight of acetyl group, and 162 is the molecular weight of AGU.

Water solubility was determined by the Soxhlet extraction method (Cao *et al*. 2016a, 2016b). To extract water-soluble BCA, the samples were refluxed for 24 h by the Soxhlet extraction using the water as the solvent. The extract was freeze-dried to obtain the water-soluble BCA product.

Field emission scanning electron microscopy (FE-SEM)

The morphological structure of the original BC and acetylated BC were obtained from SEM analysis. The freeze-dried samples were fixed using double-sided carbon tape, ion sputter-coated with gold-palladium alloy (SCD 040, Balzers AG Co., Balzers, Schaan, Liechtenstein), and analyzed using a JSM-7800F microscope (JEOL Co., Tokyo, Japan) at 15 kV. The image analysis was performed using Image J software version 1.48 (National Institutes of Health, Bethesda, MD, USA).

FTIR analysis

The FTIR spectra were obtained using a Thermo Nicolet Nexus spectrophotometer (Nicolet Instrument Corporation, Madison, WI, USA). The samples were first ground and pressed with KBr. The data were recorded over the range 400 cm^{-1} to 4000 cm^{-1} in absorbance mode with 64 scans per spectrum at a resolution of 4 cm^{-1}.

^{13}C Cross polarization magic angle spinning nuclear magnetic resonance (CP/MAS NMR) spectroscopy

The chemical molecular structures of the samples were further validated using solid-state ^{13}C CP/MAS NMR spectroscopy using a Bruker AV 400 spectrometer (Bruker

Corporation, Karlsruhe, Germany) at room temperature with a 4-mm MAS probe at 100 MHz, the contact time during the CP was 2 ms. The frequency for protons and carbons used were 400.17 and 100.6 MHz, respectively.

XRD analysis

The crystallinity of samples was analyzed using a Bruker Advance D8 X-ray diffractometer in transmission model (Bruker Corporation, Karlsruhe, Germany) with Ni-filtered Cu Kα radiation (λ = 0.154 nm) at 40 kV and 40 mA. The diffraction data were collected from 2θ = 5° to 40° at a scanning rate of 5°/min.

The crystalline index (CrI) was calculated according to Segal′s empirical method (Segal *et al.* 1962),

$$CrI = (I_{200} - I_{am}) / I_{200} \times 100 \quad (3)$$

where I_{200} corresponds to the maximum diffraction intensity of the 200 crystalline plane diffraction, and the amorphous (I_{am}) contribution at 2θ = 18°.

TGA

The thermal properties of native BC and BCA samples were determined using a TGA 4000 analyzer (PerkinElmer, Waltham, MA, USA). *Ca.* 5 mg of the BC powder was placed in an open alumina crucible, then heated at the rate of 20 °C/min and temperature range of 50 °C to 800 °C; the tests were performed under a nitrogen flow of 20 mL/min.

RESULTS AND DISCUSSION

The Effects of the Reaction Parameters on Acetylation of BC

The reaction variables' optimization towards DS value in acetylation of BC was performed for both heterogeneous and homogeneous reactions. The correlation between the reaction conditions and the DS values is presented in Table 1.

For heterogeneous reaction, the BC was kept as suspension, and NMIM catalyst was added along with an excess of Ac_2O. Herein, the catalyst concentration, Ac2O amount, reaction temperature, and reaction time were evaluated for each sample. As shown in Table 1 (Left column for BCA-HE), the NMIM concentration was optimized at the range of 0.1 mM to 0.5 mM, where the DS value approached its maximum value at 0.3 mM catalyst concentration. The DS increased with increased amount of Ac_2O from 8 mL to 10 mL, but no further obvious changes were recorded when adding up to 12 mL. The reactions were managed by changing the temperature from 50 °C to 90 °C, and the DS value reached its maximum record at 70 °C. In addition, the DS value also increased along with more reaction time from 180 min to 300 min, while a slight decline in its values was recorded after 300 min reaction time.

In addition, the homogenous reaction conditions were also evaluated. The results (Table 1, Right column for BCA-HE) showed that the DS values of the corresponding samples from BCA-HO increased from 0.83 to 1.50 at an NMIM concentration range from 0.1 mM to 0.4 mM, and then decreased at a higher NMIM concentration. The DS values increased extensively when the amount of Ac_2O was adjusted from 1.0 mL to 3.0 mL. In addition, the DS value increased along with more reaction time from 30 min to 120 min, but decreased with prolonged time. Clearly, the DS value reached its maximum at 40 °C, and then declined at higher temperature. Accordingly, it may be concluded that the stability of NMIM declined with the increasing of temperature in the DMAc/LiCl system.

Table 1. DS Values of BCA-HE and BCA-HO Obtained Under Various Reaction Conditions

BCA-HE							BCA-HO					
No.	NMIM (mM)	Ac_2O (mL)	*T* (°C)	Time (min)	DS		No.	NMIM (mM)	Ac_2O (mL)	*T* (°C)	Time (min)	DS
1	0.1	10	70	300	0.31		1	0.1	3	40	120	0.83
2	0.2	10	70	300	0.63		2	0.2	3	40	120	0.94
3	0.3	10	70	300	0.95		3	0.3	3	40	120	1.13
4	0.4	10	70	300	0.89		4	0.4	3	40	120	1.5
5	0.5	10	70	300	0.8		5	0.5	3	40	120	1.25
6	0.3	8	70	300	0.65		6	0.4	1	40	120	1.07
7	0.3	9	70	300	0.80		7	0.4	2	40	120	1.19
8	0.3	10	70	300	0.95		8	0.4	3	40	120	1.5
9	0.3	11	70	300	0.92		9	0.4	4	40	120	1.33
10	0.3	12	70	300	0.94		10	0.4	5	40	120	1.30
11	0.3	10	50	300	0.51		11	0.4	3	20	120	1.12
12	0.3	10	60	300	0.63		12	0.4	3	30	120	1.23
13	0.3	10	70	300	0.95		13	0.4	3	40	120	1.5
14	0.3	10	80	300	0.83		14	0.4	3	50	120	1.29
15	0.3	10	90	300	0.79		15	0.4	3	60	120	1.19
16	0.3	10	70	180	0.60		16	0.4	3	40	30	0.4
17	0.3	10	70	240	0.74		17	0.4	3	40	60	0.77
18	0.3	10	70	300	0.95		18	0.4	3	40	90	1.38
19	0.3	10	70	360	0.88		19	0.4	3	40	120	1.5
20	0.3	10	70	420	0.80		20	0.4	3	40	150	1.27

In previous research findings, NMIM has been applied as an effective Lewis base catalyst for acetylation of the hydroxyl groups in the presence of Ac_2O, such as in neutral sugars, alditol, and plant polysaccharides (McGinnis 1982; Lu and Ralph 2003; Wu *et al*. 2011; Zhang *et al*. 2012a; Nawaz *et al*. 2013; Pires *et al*. 2015; Zhang *et al*. 2016). Its catalytic activity was shown to be roughly 4×10^2 times greater than pyridine (Connors and Pandit 1978). Therefore, clearly, NMIM catalyzed reactions are considered to be more effective due to their chemical nature. A catalytic mechanism was proposed in previous reports (Connors and Pandit 1978; Nawaz *et al.* 2013). Based on the reaction mechanism, the NMIM first activates the carbonyl carbon of acetic anhydride, and then forms the intermediate, 1-acyl-3-methylimidazolium ion, which is further attacked by the oxygen of hydroxyl groups of cellulose in a nucleophilic way.

In this study, NMIM was used as a catalyst to prepare the BCA under both solvent-free and DMAc/LiCl system. Under an optimized reaction condition, the highest DS value obtained for BCA-HE and BCA-HO was recorded as 0.95 and 1.5, respectively, where a low DS value indicated a partial acetylation during its reaction. Actually, the DS value catalyzed by NMIM in this study was recorded as a low value in comparison to those reported from other catalysts, such as iodine and organic acid (Li *et al*. 2009; Hu *et al*. 2011; Ávila Ramírez *et al*. 2016a,b). However, this DS value was much lower than the DS value (≈ 3) obtained using the traditional H_2SO_4 as catalyst (Cerqueira *et al*. 2007; Barud *et al*. 2008).

It is worth noting that imidazolium ILs have been used and functioned simultaneously as a solvent and a catalyst, or only as a "quasi-homogeneous" catalyst for the acetylation of cellulose, where the corresponding DS values showed a wide range due to various compositions of ILs being designed (Cao *et al*. 2007; Karatzos *et al*. 2012; Sun *et al*. 2013; Tian *et al*. 2014; Cao *et al*. 2016a; Pang *et al*. 2016; Olsson and Westman 2017; Asaadi *et al*. 2018).

In addition, a relatively higher DS value can be achieved from the homogeneous reaction than that from heterogeneous processing. The homogeneous acetylation of cellulose has shown some distinct advantages over the heterogeneous reaction due to a relatively low temperature and a short time period in reaction. This may be attributed to the disruption of cellulose crystalline structure by dissolving in DMAc/LiCl (Lima *et al*. 2011) and a synergistic role functioned by both NMIM and LiCl (Hagiwara *et al*. 2006). Compared to the previous homogeneous reaction in the DMAc/LiCl system without catalyst (Lima *et al*. 2011), a high temperature (> 100 °C) is usually required for the acetylation of BC. Further, the requisite amount of Ac_2O was actually higher in the heterogeneous reaction because the Ac_2O served as both an acetylation reagent and as a solvent. Meanwhile, the continued swelling of the dry cellulose occurred by adsorption of Ac_2O at the beginning of the heterogeneous reaction. In fact, the elevated temperature would significantly increase the swelling and diffusion rate of reagents in the cellulose. However, an excessive temperature or a prolonged reaction time can directly result in a hydrolysis of the ester groups, which was a similar result with other catalysts in early reports (Hu *et al*. 2011; Ávila Ramírez *et al*. 2016b).

Clearly, the reaction catalyzed by NMIM was truly managed under a mild condition, which would be helpful as a means to tailor the BCA at a low DS value ranging from 0.31 to 0.95 in the heterogeneous system or a DS value from 0.4 to 1.5 in the homogeneous system through controlling the reaction conditions. This study suggested that the NMIM would possibly serve as an adaptive catalyst for producing low DS BCA.

The previous reports have demonstrated that the solubility of the CA in water or in some organic solvents was somehow linked with its DS value. In general, the CA material

can only be dissolved in chloroform solvent when its DS value is higher than 2.8. When its DS value was adjusted in the range of 2.0 to 2.5, the CA material can be well dissolved in some organic solvents, such as acetone, dioxane, and methyl acetate (Fischer *et al*. 2008; Pang *et al*. 2016). Interestingly, the CA can even be dissolved in water if a much lower DS value was obtained in the range of 0.3 to 1.46 (Cao *et al*. 2008; Pang *et al*. 2016). Therefore, the water solubility of BCA at low DS values was further evaluated. From Table 2, the tested BCA-HE samples with a DS value from 0.52 to 0.95 showed solubility in H_2O, and the BCA-HO samples with a low DS value that ranged from 0.55 to 1.09 can also be dissolved in H_2O, whereas the BC and RBC showed no water solubility. The water solubility of the CA is commonly considered an important characteristic required in a variety of applications, such as film coating, thickening, lubricating, stabilizing, *etc*. (Buchanan *et al*. 1991; Wheatley 2007; Cao *et al*. 2008; Konwarth *et al*. 2013; Cao *et al*. 2016a). Despite its potential applications, the preparation of water-soluble CA is a relatively complex process that involves a conventional two-step design. Firstly, cellulose with a relatively low degree of polymerization value should be acetylated, and then, the obtained CA was subsequently subjected to a deacetylation process by a complicated hydrolysis process in an acidic media (Pang *et al*. 2016). Recently, the water solubility of CA has been successfully developed in a direct preparation using ionic liquid as catalyst (Cao *et al*. 2008; Pang *et al*. 2016). In this study, the water-soluble CA can be achieved both in heterogeneous and homogeneous reactions using a simple NMIM-catalyzed process.

Table 2. Water Solubility of BCA-HO and BCA-HE with Various DS Values

DS (BCA-HO)	Solubility[a] in H_2O	DS (BCA-HE)	Solubility[a] in H_2O
1.5	-	0.95	+
1.32	-	0.82	+
1.23	-	0.71	+
1.12	-	0.64	+
1.09	+	0.52	+
0.96	+	0.42	-
0.68	+		
0.55	+		
0.41	-		

[a] + Soluble and - Insoluble

Characterization

FE-SEM

The morphologies of original BC and BCA were analyzed by SEM (Fig. 1). The typical morphology of original BC was made up of high aspect ratio nanofibers with mean diameters of approximately 30 nm to 50 nm (Fig. 1a), the fibrous were arranged in a compact, disorderly form. In addition, the microfibrils that were randomly interconnected formed a microporous and three-dimensional network structure. These characteristics of original BC structure are in accordance with those previously described by Lee *et al*. (2015) and Du *et al*. (2018).

In the authors' observation, the ultrastructure of BCA-HE (DS = 0.95) samples showed a similar fibrous arrangement and microporous structure to that of original BC, where no visible damage on its fibril surface was observed. In addition, the diameter of cellulose from BCA-HE samples was also approximately similar to that of the original BC (Fig. 1b). These observations indicated that the procedure of acetylated modification at a low DS value did not noticeably alter its ultrastructure and only displayed some OH groups

on the surface or in the disordered domains of BC (Ávila Ramírez *et al*. 2016b). The morphology of a regenerated bacterial cellulose (RBC) sample treated with DMAc/LiCl solvent and precipitated using the deionized water was also analyzed by SEM. The original fibrous structure could not be retained for RBC (Lima *et al*. 2011). Further, the heterogeneous and rough surface-layered structure was then generated, where its morphology was similar to those from the regenerated cellulose reported in earlier studies. In this process, the hydrogen bonds of cellulose chains were broken down by DMAc/LiCl dissolution. However, the dissolved cellulose chains can be recovered due to their hydrogen bonding ability, which led to the formation of a layered structure by self-reassembling of microfibrils after the water was added to the solution (Ass *et al*. 2006a; Xia *et al*. 2014, 2015; Zhou *et al.* 2016). As presented in Fig. 1d, after homogeneous acetylation, the morphology of BCA-HO was clearly different from that of original BC and BCA-HE. The fibril bundles were formed by aggregated microfibrils, where the diameter of its bundles was larger (120 nm, arrows in Fig. 1d) than that of the native BC and BCA-HE with a sponge-like porous structure on the surface due to a random interaction with its fibril bundles.

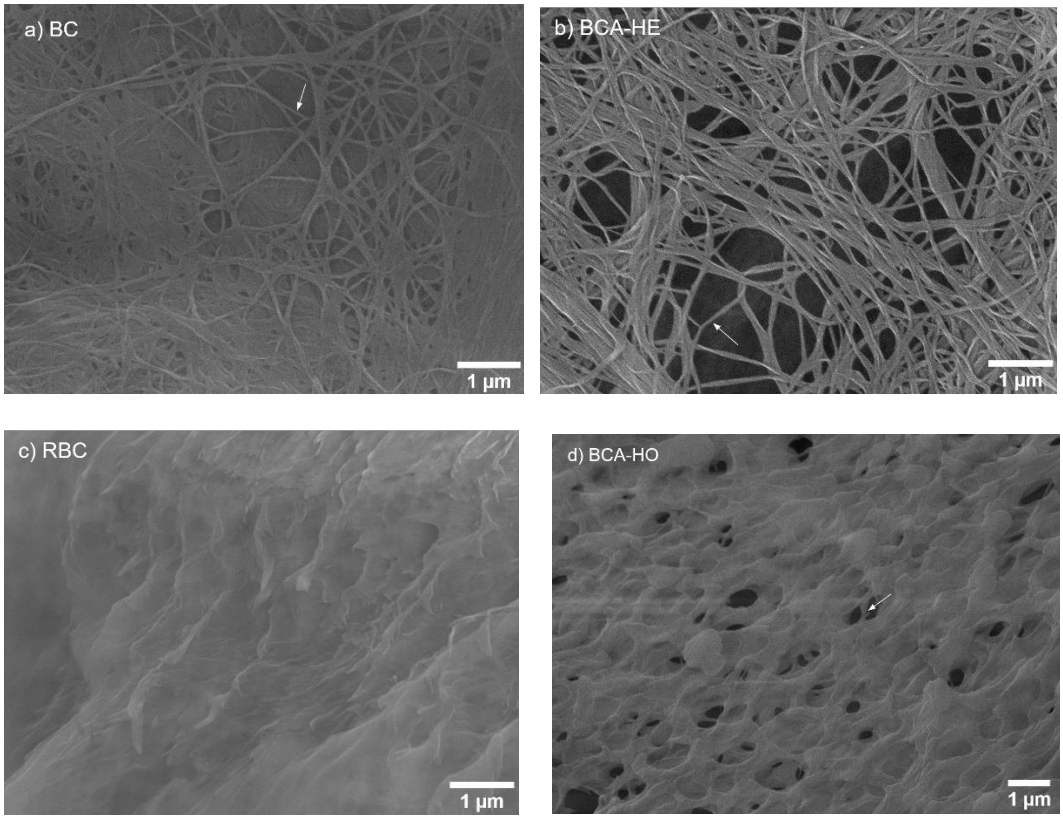

Fig. 1. FE-SEM images of (a) original BC, the arrows point to diameters of microfibrils that were 30 nm; (b) BCA-HE (DS 0.95), the diameter of microfibrils was 38 nm; (c) RBC (by DMAc/LiCl dissolving and water precipitation); and (d) BCA-HO (DS 1.5), the diameters of microfibrils were 120 nm. (a, b, and c) with 15,000× magnification; and (d) 10000× magnification

FTIR analysis

The FTIR spectroscopy is the most convenient method for the elucidation of structural features of biomacromolecules. Figures 2a and 2b depict the FTIR spectra of BCA-HE and BCA-HO samples at different DS values, respectively. As typical of cellulose, the absorbance values of BC at 3353 cm^{-1} and 2900 cm^{-1} corresponded to the

O-H and C-H bonds stretching, respectively. Interestingly, at a comparable DS value of 0.95 for BCA-HE and 0.96 for BCA-HO, the adsorption intensity of BCA-HE was higher than BCA-HO. A possible reason is that the OH in the BCA-HE was not destroyed, while OH in the BCA-HO was destroyed and reconstructed. The peak at 1642 cm^{-1} was attributed to the H-O-H bending of the absorbed water. The peak at 1152 cm^{-1} was ascribed to -C-O antisymmetric bridge stretching. The peak at 1059 cm^{-1} was ascribed to -C-O stretching vibration of pyranose ring, and the absorbance at 899 cm^{-1} was attributed to that of the β-glucosidic linkages between the AGU (Cao *et al*. 2007; Sun *et al*. 2013; Chen *et al*. 2016).

The FTIR spectra of acetylated cellulose BCA-HE and BCA-HO indicated new peaks (1745, 1370, and 1238 cm^{-1}), which were assigned to the acetyl groups. Therefore, the acetylation reaction was confirmed, where the peaks at 1745 cm^{-1} corresponded to the carbonyl C=O stretching vibration, 1370 cm^{-1} attributed to C-H bending vibration, and 1238 cm^{-1} was assigned to the C-O stretching vibration of the acetate groups. Moreover, along with the increased DS values, these peak intensities also increased, and the intensity of H-O bending vibration (1642 cm^{-1}) was reduced, indicating the extensive acetylation reaction. The absence of absorption peak at 1700 cm^{-1} for a carboxylic group indicated that the product was also free of any acetic acid byproduct.

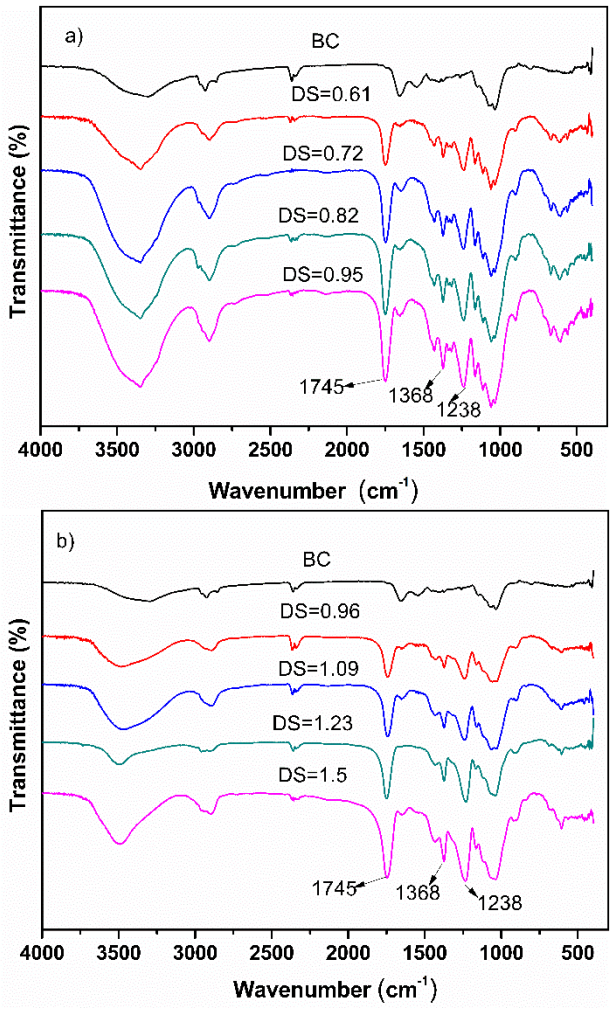

Fig. 2. FTIR spectra of (a) original BC and BCA-HE with various DS values; and (b) original BC and BCA-HO with different DS values

^{13}C CP/MAS NMR spectra

Figure 3 presents the ^{13}C CP/MAS NMR spectra for original BC, the acetylated BCA-HE, and BCA-HO samples with a DS value of 0.95 and 1.5, respectively. The characteristic peaks of original BC were found in the region between 50 ppm to 110 ppm. The resonance peak at 103.6 ppm was assigned to the C-1. The peaks at 87.7 and 82.8 ppm were related to the C-4 of crystalline (C4D) and amorphous cellulose (C4U), respectively. The peaks between 70 ppm to 80 ppm were attributed to cluster C-2, C-3, and C-5, which had overlapped to some extent and were difficult to distinguish from each other. The peaks at 64.2 ppm and 60.7 ppm were C-6 of crystalline (C6D) and amorphous region (C6U) (Hult *et al*. 2002; Hu *et al*. 2011; Ávila Ramírez *et al*. 2016b).

With respect to the spectra of BCA-HE and BCA-HO samples, the two new peaks found at 169.3 ppm and 19.2 ppm belong to -C=O and -CH_3 in acetyl group, which indicated the occurrence of the acetylation reaction (Yamamoto *et al*. 2006; Li *et al*. 2009; Hu *et al*. 2011; Ávila Ramírez *et al*. 2016b). According to the intensity of new peaks, the extent of acetylation for tested samples of BCA-HO was higher than that of BCA-HE, which was consistent with their DS values. Further, the decrease in intensities of peaks at 103.6 ppm (C-1), 70 to 80 ppm (C-2, C3, and C-5), and 64.2 ppm (C-6) occurred with the increase of peak intensity at 169.3 ppm and 19.2 ppm, suggesting that the -OH groups almost simultaneously associated with these carbons undergoing an acetylation reaction.

Based on the analysis of BC and BCA-HE sample spectra, the peak intensities of C4 and C6 regions presented a slight decrease due of its low DS value (0.95). With RBC spectral analysis, the resonances of C4 and C6 crystalline regions decreased noticeably, while the disordered regions slightly increased. This clearly indicated that the crystalline structure of the cellulose was disrupted due to the DMAc/LiCl dissolving. From the BCA-HO sample spectra, both the amorphous and crystalline regions of C4 almost disappeared, and the crystalline region of C6 was still partly retained. It can be deduced that the acetylation more easily occurs at the C4 region than at the C6 region, and the reaction occurred primarily in the amorphous region.

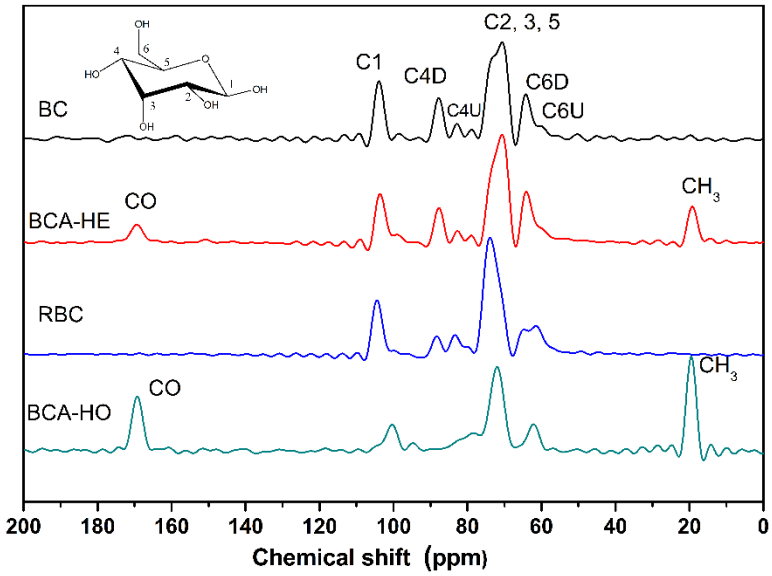

Fig. 3. Solid-state ^{13}C CP/MAS NMR spectra of original BC, BCA-HE (DS 0.95), RBC, and BCA-HO (DS 1.5)

Thermal analysis

The thermal behavior was analyzed and evaluated by the TG and DTG curves for each sample of original BC and acetylated BC. As shown in Fig. 4a, the TG and DTG curves of BC and the acetylated BC revealed a similar weight loss and presented typical cellulose pyrolysis behavior, which can further be divided into three different phases: dehydration, depolymerization, and decomposition of glycosyl units.

At the water desorption stage in the temperature range of 50 °C to 200 °C, all samples exhibited a little bit of weight loss due to the freeze-dried tested samples. Among them, the BCA-HO had the smallest weight loss. Hence, the BCA-HO samples at DS 1.5 were more hydrophobic than that of the original cellulose, as well as the BCA-HE sample at DS 0.95. Clearly, the rapid weight losses were a result of degradation of the main cellulose skeleton. During this stage, the crystalline region started to be destroyed, and simultaneously, its polymer structure was then decomposed. The onset temperatures were considered to start at 344.6 °C, 290.4 °C, and 288.3 °C for original BC, BCA-HE, and BCA-HO, respectively. These results indicated that the original BC was typically thermostable compared to BCA. It is said that this observed response is generally attributable to the decrease of crystallinities after acetylation, and it may also be associated with a high instability of the acetyl groups that was introduced to the cellulose structure. A similar behavior was also reported in other investigations (Cao *et al*. 2007; Ávila Ramírez *et al*. 2017). However, in the iodine catalyzed BC acetylation, the acetylated BC resulted in a higher thermal stability than that of original BC (Hu *et al*. 2011).

The thermal characteristics of the evaluated samples were further observed using DTG measurements (Fig. 4b). All of those measured samples exhibited a large endothermic peak, and their endothermic peaks in DTG thermograms for acetylated samples were smaller than that of original cellulose. The maximum decomposition temperature for the samples of BC, BCA-HE, and BCA-HO was recorded at 418.7 °C, 379.6 °C, and 362.8 °C, respectively. These findings further indicated that the degree of crystallinity was lower than that of original BC.

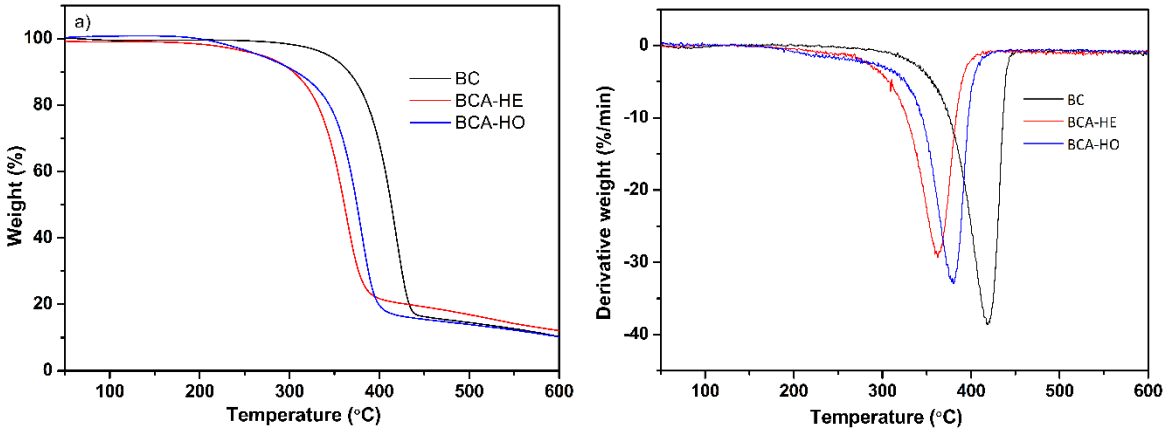

Fig. 4. TG (a) and DTG (b) data of BC, BCA-HE (DS 0.95), and BCA-HO (DS 1.5)

XRD analysis

The impact of chemical modification on the crystalline structures of the cellulose nanofibers was further evaluated using XRD analysis. The XRD profiles of original BC, RBC, and BCA samples are shown in Fig. 5. The original BC sample showed three well-defined diffraction peaks centered approximately at 2θ values of 14.6°, 16.8°, and 22.7°, corresponding to the ($\bar{1}$10), (110), and (200) lattice planes. The corresponding crystallinity

index (CrI) obtained was 91.6%. These characteristic peaks can be identified as a cellulose-I crystalline structure (Li *et al*. 2009; Hu *et al*. 2011; Ávila Ramírez *et al*. 2017). Compared to the original BC, the intensities of three peaks of BCA-HE (DS 0.95) decreased dramatically, and the CrI decreased to 86.5%. Meanwhile, its peak at 22.8° of RBC and BCA-HO (DS 1.5) completely disappeared. These changes indicated that the crystalline regions of the original BC were partially destroyed by the acetylation process, where the reaction occurred beyond the surface of the cellulose microfibrils. Further, the crystallinity of BC decreased during the dissolution and homogeneous processes. Compared with that of the original BC, the acetylated BCA-HE and BCA-HO presented a relatively low degree of crystallinity. One of the reasons for this was that the hydrogen bonds of cellulose were actually broken by a substitution of the -OH groups by acetyl groups. Additionally, the solvent destruction may play an important role for the BCA-HO reaction. Some similar observations were also reported in catalyst derivatization (Hu *et al*. 2011; Lima *et al*. 2011). It has been suggested that there may exist a correlation between the diffraction patterns of acetylated cellulose and its DS value. There were no detectable changes at low DS value (< 0.38) in the intensities of characteristic peaks compared to that of the origin cellulose (Agustin *et al*. 2016), but when the product was a type of cellulose triacetate, the new peak will possibly present with a change at 2θ value of 26° (Ávila Ramírez *et al*. 2016b).

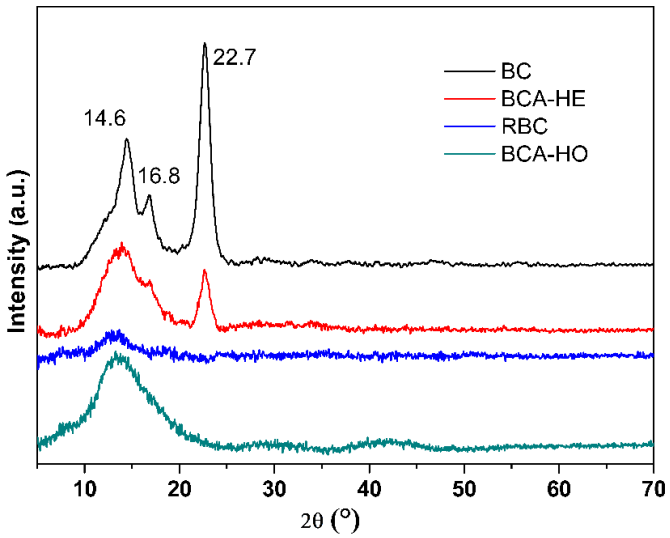

Fig. 5. The XRD patterns of original BC, BCA-HE (DS 0.95), RBC, and BCA-HO (DS 1.5)

CONCLUSIONS

1. The bacterial cellulose acetate (BCA) of low degree of substitution (DS) values could be prepared both in heterogeneous and homogeneous systems using N-methylmidazole (NMIM) as a catalyst. The DS values ranging from 0.31 to 0.95 for BCA-HE and from 0.4 to 1.5 for BCA-HO could be obtained by controlling the reaction conditions. The water solubility can be achieved when the DS value was lower than 0.95 and 1.09 for BCA-HE and BCA-HO, respectively. The reaction was indeed mild and environmentally benign.
2. The highest DS value (1.5) for homogeneous acetylation of BC could be obtained at relatively low temperature (40 °C) and a short time (120 min), while the highest DS value (0.95) could be achieved at a high temperature (70 °C) and a long time (300 min)

for heterogeneous reaction. The homogeneous acetylation has shown advantages over the heterogeneous reaction.

3. The new characteristic peaks (1745, 1370, and 1238 cm^{-1}) in the FTIR and the peaks (169.3 and 19.2 ppm) in the ^{13}C NMR confirmed a successful acetylation of BC. XRD showed that the CrI had slight decreases from 91.6 (BC) to 86.5 % (BCA-HE), while the peaks of BCA-HO in the (200) plane disappeared as a consequence of dissolution in DMAc/LiCl. Through SEM observation, the surface morphologies of the BCA-HO nanofibrils exhibited an obvious alternation, but the BCA-HE remained in its original structure. The thermostability of BCA moderately decreased *via* TG analysis, the maximum decomposition temperature for the samples of BC, BCA-HE, and BCA-HO was recorded at 418.7 °C, 379.6 °C, and 362.8 °C, respectively.

ACKNOWLEDGMENTS

This work was financially supported by the National Key R & D Program of China (2018YFE0107100), the Startup Foundation of Jiangsu University (11JDG110), the Priority of Academic Program Development of Jiangsu Higher Education Institutions (PAPD 4013000011), the National Natural Science Foundation of China (31772529), the Jiangsu Key Laboratory for Biomass Energy and Material (JSBEM201807), and the Postdoctoral Science Foundation of China (2018T110447).

REFERENCES CITED

Agustin, M. B., Nakatsubo, F., and Yano, H. (2016). "The thermal stability of nanocellulose and its acetates with different degree of polymerization," *Cellulose* 23(1), 451-464. DOI: 10.1007/s10570-015-0813-x

Amin, M., Abbas, N. S., Hussain, M. A., Edgar, K. J., Tahir, M. N., Tremel, W., and Sher, M. (2015). "Cellulose ether derivatives: A new platform for prodrug formation of fluoroquinolone antibiotics," *Cellulose* 22(3), 2011-2022. DOI: 10.1007/s10570-015-0625-z

Asaadi, S., Kakko, T., King, A. W. T., Kilpeläinen, I., Hummel, M., and Sixta, H. (2018). "High-performance acetylated ioncell-F fibers with low degree of substitution," *ACS Sustainable Chemistry and Engineering* 6(7), 9418-9426. DOI: 10.1021/acssuschemeng.8b01768

Ashori, A., Babaee, M., Jonoobi, M., and Hamzeh, Y. (2014). "Solvent free acetylation of cellulose nanofibers for improving compatibility and dispersion," *Carbohydrate Polymers* 102, 369-375. DOI: 10.1016/j.carbpol.2013.11.067

Ass, B. A. P., Belgacem, M. N., and Frollini, E. (2006a). "Mercerized linters cellulose: Characterization and acetylation in N, N-dimethylacetamide/lithium chloride," *Carbohydrate Polymers* 63(1), 19-29. DOI: 10.1016/j.carbpol.2005.06.010

Ass, B. A. P., Ciacco, G. T., and Frollini, E. (2006b). "Cellulose acetates from linters and sisal: Correlation between synthesis conditions in DMAc/LiCl and product properties," *Bioresource Technology* 97(14), 1696–1702. DOI: 10.1016/j.biortech.2005.10.009

Ass, B. A. P., Frollini, E., and Heinze, T. (2004). "Studies on the homogeneous acetylation of cellulose in the novel solvent dimethyl sulfoxide/tetrabutylammonium fluoride trihydrate," *Macromolecular Bioscience* 4(11), 1008-1013. DOI:

10.1002/mabi.200400088

Ávila Ramírez, J. A., Gómez Hoyos, C., Arroyo, S., Cerrutti, P., and Foresti, M. L. (2016a). "Naturally occurring α-hydroxy acids: Useful organocatalysts for the acetylation of cellulose nanofibers," *Current Organocatalysis* 3(2), 161–168. DOI: 10.2174/2213337202666150428232503

Ávila Ramírez, J. A., Gómez Hoyos, C., Arroyo, S., Cerrutti, P., and Foresti, M. L. (2016b). "Acetylation of bacterial cellulose catalyzed by citric acid: Use of reaction conditions for tailoring the esterification extent," *Carbohydrate Polymers* 153, 686–695. DOI: 10.1016/j.carbpol.2016.08.009

Ávila Ramírez, J. A., Fortunati, E., Kenny, J. M., Torre, L., and Foresti, M. L. (2017). "Simple citric acid-catalyzed surface esterification of cellulose nanocrystals," *Carbohydrate Polymers* 157, 1358-1364. DOI: 10.1016/j.carbpol.2016.11.008

Barud, H. S., Araújo, A. M. D., Santos, D. B., Assunção, R. M. N. D., Meireles, C. S., Cerqueira, D. A., Filho, G. R., Ribeiro, C. A., Messaddeq, Y., and Ribeiro, S. J. L. (2008). "Thermal behavior of cellulose acetate produced from homogeneous acetylation of bacterial cellulose," *Thermochimica Acta* 471(1-2), 61-69. DOI: 10.1016/j.tca.2008.02.009

Buchanan, C. M., Edgar, K. J., and Wilson, A. K. (1991). "Preparation and characterization of cellulose monoacetates: The relationship between structure and water solubility," *Macromolecules* 24(11), 3060-3064. DOI: 10.1021/ma00011a005

Cao, J., Sun, W. W., Lu, C. H., Zhou, Z. H., Zhang, X. X., and Yuan, G. P. (2016a). "Water-soluble cellulose acetate from waste cotton fabrics and the aqueous processing of all-cellulose composites," *Carbohydrate Polymers* 149, 60-67. DOI: 10.1016/j.carbpol.2016.04.086

Cao, J., Sun, X. W., Zhang, X. X., and Lu, C. H. (2016b). "Homogeneous synthesis of Ag nanoparticles-doped water-soluble cellulose acetate for versatile applications," *International Journal of Biological Macromolecules* 92, 167-173. DOI: 10.1016/j.ijbiomac.2016.06.092

Cao, Y., Li, H. Q., Zhang, Y., Zhang, J., and He, J. S. (2008). "Synthesis of cellulose acetates with low degree of substituent and their water solubility," *Chemical Journal of Chinese Universities* 29(10), 2115-2117. DOI: 10.1007/978-3-540-77072-5_3

Cao, Y., Wu, J., Meng, T., Zhang, J., He, J. S., Lia, H. Q., and Zhang, Y. (2007). "Acetone-soluble cellulose acetates prepared by one-step homogeneous acetylation of cornhusk cellulose in an ionic liquid 1-allyl-3-methylimidazolium chloride (AmimCl)," *Carbohydrate Polymers* 69(4), 665-672. DOI: 10.1016/j.carbpol.2007.02.001

Cerqueira, D. A., Filho, G. R., and Meireles, C. D. S. (2007). "Optimization of sugarcane bagasse cellulose acetylation," *Carbohydrate Polymers* 69(3), 579-582. DOI: 10.1016/j.carbpol.2007.01.010

Cetin, N. S., Tingaut, P., Ozmen, N., Henry, N., Harper, D., Dadmun, M., and Sèbe, G. (2009). "Acetylation of cellulose nanowhiskers with vinyl acetate under moderate conditions," *Macromolecular Bioscience* 9(10), 997-1003. DOI: 10.1002/mabi.200900073

Chen, J. H., Xu, J. K., Wang, K., Cao, X. F., and Sun, R. C. (2016). "Cellulose acetate fibers prepared from different raw materials with rapid synthesis method," *Carbohydrate Polymers* 137, 685-692. DOI: 10.1016/j.carbpol.2015.11.034

Connors, K. A., and Pandit, N. K. (1978). "N-Methylimidazole as a catalyst for analytical acetylations of hydroxy compounds," *Analytical Chemistry* 50(11), 1542-1545. DOI: 10.1021/ac50033a038

Du, R. P., Zhao, F. K., Peng, Q., Zhou, Z. J., and Han, Y. (2018). "Production and characterization of bacterial cellulose produced by *Gluconacetobacter xylinus* isolated from Chinese persimmon vinegar," *Carbohydrate Polymers* 194, 200–207. DOI: 10.1016/j.carbpol.2018.04.041

Fischer, S., Thümmler, K., Volkert, B., Hettrich, K., Schmidt, I., and Fischer, K. (2008). "Properties and applications of cellulose acetate," *Macromolecular Symposia* 262(1), 89-96. DOI: 10.1002/masy.200850210

Fox, S. C., Li, B., Xu, D. Q., and Edgar, K. J. (2011). "Regioselective esterification and etherification of cellulose: A review," *Biomacromolecules* 12(6), 1956-1972. DOI: 10.1021/bm200260d

Frisoni, G., Baiardo, M., and Scandola, M. (2001). "Natural cellulose fibers: Heterogeneous acetylation kinetics and biodegradation behavior," *Biomacromolecules* 2(2), 476-482. DOI: 10.1021/bm0056409

Fu, L. N., Zhang, J., and Yang, G. (2013). "Present status and applications of bacterial cellulose-based materials for skin tissue repair," *Carbohydrate Polymers* 92(2), 1432-1442. DOI: 10.1016/j.carbpol.2012.10.071

Hagiwara, H., Inoguchi, H. Y., Fukushima, M., Hoshi, T., and Suzuki, T. (2006). "Practical aldol reaction of trimethylsilyl enolate with aldehyde catalyzed by N-methylimidazole as a Lewis base catalyst," *Tetrahedron Letters* 47(30), 5371–5373. DOI: 10.1002/chin.200645073

Hestrin, S., and Schramm, M. (1954). "Synthesis of cellulose by *Acetobacter xylinum*. II. Preparation of freeze-dried cells capable of polymerizing glucose to cellulose," *Biochemical Journal* 58(2), 345-352. DOI: 10.1007/s00706-014-1395-2

Hu, W. L., Chen, S. Y., Xu, Q. S., and Wang, H. P. (2011). "Solvent-free acetylation of bacterial cellulose under moderate conditions," *Carbohydrate Polymers* 83(4), 1575-1581. DOI: 10.1016/j.carbpol.2010.10.016

Hult, E. L., Liitiä, T., Maunu, S. L., Hortling, B., and Iversen T. (2002). "A CP/MAS 13C-NMR study of cellulose structure on the surface of refined kraft pulp fibers," *Carbohydrate Polymers* 49(2), 231-234. DOI: 10.1016/s0144-8617(01)00309-5

Isikgor, F. H., and Becer, C. R. (2015). "Lignocellulosic biomass: A sustainable platform for the production of bio-based chemicals and polymers," *Polymer Chemistry* 6(25), 4497-4559. DOI: 10.1039/C5PY00263J

Kang, H. L., Liu, R. G., and Huang, Y. (2015). "Graft modification of cellulose: Methods, properties and applications," *Polymer* 70, A1-A16. DOI: 10.1016/j.polymer.2015.05.041

Karatzos, S. K., Edye, L. A., and Wellard, R. W. (2012). "The undesirable acetylation of cellulose by the acetate ion of 1-ethyl-3-methylimidazolium acetate," *Cellulose* 19(1), 307-312. DOI: 10.1007/s10570-011-9621-0

Kim, D. Y., Nishiyama, Y., and Kuga, S. (2002). "Surface acetylation of bacterial cellulose," *Cellulose* 9(3-4), 361-367. DOI: 10.1023/a:1021140726936

Klemm, D., Heublein, B., Fink, H. P., and Bohn, A. (2005). "Cellulose: Fascinating biopolymer and sustainable raw material," *Angewandte Chemie International Edition* 44(22), 3358–3393. DOI: 10.1002/anie.200460587

Li, J., Zhang, L. P., Peng, F., Bian, J., Yuan, T. Q., Xu, F., and Sun, R. C. (2009). "Microwave-assisted solvent-free acetylation of cellulose with acetic anhydride in the presence of iodine as a catalyst," *Molecules* 14(9), 3551-3566. DOI: 10.3390/molecules14093551

Lee, C. M., Gu, J., Kaflea, K., Catchmark, J., and Kim, S. H. (2015). "Cellulose produced by *Gluconacetobacter xylinus* strains ATCC 53524 and ATCC 23768: Pellicle

formation, post-synthesis aggregation and fiber density," *Carbohydrate Polymers* 133, 270–276. DOI: 10.1016/j.carbpol.2015.06.091

Lima, G. D. M., Sierakowski, M. R., Tischer-Faria, P. C. S., and Tischer, C. A. (2011). "Characterisation of bacterial cellulose partly acetylated by dimethylacetamide/ lithium chloride," *Materials Science and Engineering C* 31, 190-197. DOI: 10.1016/j.msec.2010.08.017

Lin, N., Huang, J., Chang, P. R., Feng, J. W., and Yu, J. H. (2011). "Surface acetylation of cellulose nanocrystal and its reinforcing function in poly (lactic acid)," *Carbohydrate Polymers* 83(4), 1834-1842. DOI: 10.1016/j.carbpol.2010.10.047

Lu, F. C., and Ralph, J. (2003). "Non-degradative dissolution and acetylation of ball-milled plant cell walls: High-resolution solution-state NMR," *Plant Journal* 35(4), 535-544. DOI: 10.1046/j.1365-313X.2003.01817.x

McGinnis, G. D. (1982). "Preparation of aldononitrile acetates using N-methylimidazole as catalyst and solvent," *Carbohydrate Research* 108(2), 284-292. DOI: 10.1016/S0008-6215(00)81799-1

Nawaz, H., Pires, P. A. R., and El Seoud, O. A. (2013). "Kinetics and mechanism of imidazole-catalyzed acylation of cellulose in LiCl/N, N-dimethylacetamide," *Carbohydrate Polymers* 92(2), 997-1005. DOI: 10.1016/j.carbpol.2012.10.009

Nie, Y., Chen, C. T., and Sun, D. P. (2014). "Recent advances in bacterial cellulose," *Cellulose* 21(1), 1-30. DOI: 10.1007/s10570-013-0088-z

Olsson, C., and Westman, G. (2017). "Co-solvent facilitated in situ esterification of cellulose in 1-ethyl-3-methylimidazolium acetate," *BioResources* 12(1), 1395-1402. DOI: 10.15376/biores.12.1.1395-1402

Pang, J. H., Liu, X., Yang, J., Lu, F. C., Wang, B., Xu, F., Ma, M. G., and Zhang, X. M. (2016). "Synthesis of Highly polymerized water-soluble cellulose acetate by the side reaction in carboxylate ionic liquid 1-ethyl-3-methylimidazolium acetate," *Scientific Reports* 6, Article Number 33725. DOI: 10.1038/srep33725

Pires, P. A. R., Malek, N. I., Teixeira, T. C., Bioni, T. A., Nawaz, H., and El Seoud, O. A. (2015). "Imidazole-catalyzed esterification of cellulose in ionic liquid/molecular solvents: A multi-technique approach to probe effects of the medium," *Industrial Crops and Products* 77, 180-189. DOI: 10.1016/j.indcrop.2015.08.015

Shah, N., Ul-Islam, M., Khattak, W. A., and Park, J. K. (2013). "Overview of bacterial cellulose composites: A multipurpose advanced material," *Carbohydrate Polymers* 98(2), 1585-1598. DOI: 10.1016/j.carbpol.2013.08.018

Segal, L., Creely, J. J., Martin, A. E. J., and Conrad, C. M. (1962). "An empirical method for estimating the degree of crystallinity of native cellulose using the X-ray diffractometer," *Textile Research Journal* 29(10), 786-794. DOI: 10.1177/004051755902901003

Sheldon, R. A. (2014). "Green and sustainable manufacture of chemicals from biomass: State of the art," *Green Chemistry* 16(3), 950-963. DOI: 10.1039/C3GC41935E

Shi, Z. J., Zhang, Y., Phillips, G. O., and Yang, G. (2014). "Utilization of bacterial cellulose in food," *Food Hydrocolloids* 35, 539-545. DOI: 10.1016/j.foodhyd.2013.07.012

Sun, X. W., Lu, C. H., Zhang, W., Tian, D., and Zhang, X. X. (2013). "Acetone-soluble cellulose acetate extracted from waste blended fabrics *via* ionic liquid catalyzed acetylation," *Carbohydrate Polymers* 98, 405-411. DOI: 10.1016/j.carbpol.2013.05.089

Svensson, A., Nicklasson, E., Harrah, T., Panilaitis, B., Kaplan, D. L., Brittberg, M., and Gatenholm, P. (2005). "Bacterial cellulose as a potential scaffold for tissue engineering of cartilage," *Biomaterials* 26(4), 419-431. DOI: 10.1016/j.biomaterials.2004.02.049

Tian, D., Han, Y. Y., Lu, C. H., Zhang, X. X., and Yuan, G. P. (2014). "Acidic ionic liquid as "quasi-homogeneous" catalyst for controllable synthesis of cellulose acetate," *Carbohydrate Polymers* 113, 83–90. DOI: 10.1016/j.carbpol.2014.07.005

Wan, Y. F., An, F., Zhou, P. C., Li, Y. H., Liu, Y. D., Lu, C. X., and Chen, H. X. (2017). "Regenerated cellulose I from LiCl· DMAc solution," *Chemical Communication* 53(25), 3595-3597. DOI: 10.1039/c7cc00450h

Wang, N., Ding, E. Y., and Cheng, R. S. (2007). "Surface modification of cellulose nanocrystals," *Frontiers of Chemical Engineering in China* 1(3), 228-232. DOI: 10.1007/s11705-007-0041-5

Wheatley, T. A. (2007). "Water soluble cellulose acetate: A versatile polymer for film coating," *Drug Development and Industrial pharmacy* 33(3), 281-290. DOI: 10.1080/03639040600683469

Wu, J., Li, M. H., Lin, J. P., and Wei, D. Z. (2011). "Determination of dihydroxyacetone and glycerol in fermentation process by GC after N-methylimidazole catalyzed acetylation," *Journal of Chromatographic Science* 49(5-6), 375-378. DOI: 10.1093/chromsci/49.5.375

Wu, J., Zhang, J., Zhang, H., He, J. S., Ren, Q., and Guo, M. L. (2004). "Homogeneous acetylation of cellulose in a new ionic liquid," *Biomacromolecules* 5(2), 266-268. DOI: 10.1021/bm034398d

Xia, X. L., Yao, Y. B., Gong, M. F., Wang, H. P., and Zhang, Y. M. (2014). "Rheological behaviors of cellulose/[BMIM]Cl solutions varied with the dissolving process," *Journal of Polymer Research* 21, Article Number 512. DOI: 10.1007/s10965-014-0512-6

Xu, A. R., Cao, L. L., and Wang, B. J. (2015). "Facile cellulose dissolution without heating in [C_4mim][CH_3COO]/DMF," *Carbohydrate Polymers* 125, 249-254. DOI: 10.1016/j.carbpol.2015.02.045

Yamamoto, H., Horii, F., and Hirai, A. (2006). "Structural studies of bacterial cellulose through the solid-phase nitration and acetylation by CP/MAS 13C NMR spectroscopy," *Cellulose* 13(3), 327-342. DOI: 10.1007/s10570-005-9034-z

Zhang, A. P., Liu, C. F., Sun, R. C., Xie, J., and Chen, X. Y. (2012a). "Homogeneous acylation of eucalyptus wood at room temperature in dimethyl sulfoxide/N-methylimidazole," *Bioresoure Technology* 125, 328-331. DOI: 10.1016/j.biortech.2012.08.131

Zhang, X. M., Liu, X. Q., Zheng, W. G., and Zhu, J. (2012b). "Regenerated cellulose/graphene nanocomposite films prepared in DMAC/LiCl Solution," *Carbohydrate Polymers* 88(1), 26-30. DOI: 10.1016/j.carbpol.2011.11.054

Zhang, X. X., Zhang, W., Tian, D., Zhou, Z. H., and Lu, C. H. (2013). "A new application of ionic liquids for heterogeneously catalyzed acetylation of cellulose under solvent-free conditions," *RSC Advances* 3(21), 7722-7725. DOI: 10.1039/C3RA21894E

Zhou, X. M., Lin, X. X., White, K. L., Lin, S., Wu, H., Cao, S. L., Huang, L. L., and Chen, L. H. (2016). "Effect of the degree of substitution on the hydrophobicity of acetylated cellulose for production of liquid marbles," *Cellulose* 23(1), 811-821. DOI: 10.1007/s10570-015-0856-z

Zhu, S. D., Wu, Y. X., Chen, Q. M., Yu, Z. N., Wang, C. W., Jin, S. W., Ding, Y. G., and Wu. G. (2006). "Dissolution of cellulose with ionic liquids and its application: A mini-review," *Green Chemistry* 8(4), 325–327. DOI: 10.1039/b601395c

Article submitted: October 7, 2019; Peer review completed: March 21, 2020; Revised version received: March 27, 2020; Accepted: March 28, 2020; Published: April 1, 2020.
DOI: 10.15376/biores.15.2.3688-3706